

Preparation, kinetics and microstructures of well-defined PS-*b*-PS/Bd diblock copolymers via RAFT miniemulsion polymerization

Zhenxi Wang · Qinghua Zhang · Xiaoli Zhan ·
Fengqiu Chen · Guohua Rao · Jihai Xiong

Received: 17 July 2013 / Accepted: 2 October 2013 / Published online: 14 October 2013
© Springer Science+Business Media Dordrecht 2013

Abstract Well-defined PS-*b*-PS/Bd diblock copolymers were synthesized via reversible addition-fragmentation chain transfer (RAFT) miniemulsion polymerization instead of anionic polymerization, which was environmental friendly, energy and cost saving for most monomers. In order to precisely design styrene/butadiene block with targeted composition profile given the feeding program, binary monomers RAFT miniemulsion polymerization kinetic models were formulated. In butadiene RAFT seeded miniemulsion polymerization, it was well performed, and the RAFT equilibrium constant between butadiene and 1-phenylethyl phenyldithioacetate (PEPDTA) was estimated to be $18.3 L/mol \times s$ at 70 °C. Furthermore, the modeling curves could well predict styrene/butadiene RAFT miniemulsion polymerization kinetics, including monomers conversion, volume fraction of monomers, number-average molecular weight and composition. The copolymers were characterized by fourier translation infrared spectroscopy (FT-IR), hydrogen nuclear magnetic resonance spectroscopy (1H -NMR), transmission electron microscopy (TEM), and differential scanning calorimetry (DSC). FT-IR and 1H -NMR results indicated that the microstructure of the polymer was mainly 1, 4-*trans* butadiene with small amount of 1, 2-units. Microphase morphologies of the copolymers were lamellar, cylinder and disordered phase by TEM, which was identical to self-consistent field calculations. And thermal property results showed that glass transition behaviors were corresponding with their microphase separation, sequence length and composition from DSC.

Keywords Kinetics · Microstructures · Reversible addition-fragmentation chain transfer (RAFT) · Miniemulsion polymerization

Introduction

Styrene-butadiene copolymers were important parts of the polymer materials, which was widely used in rubber, high performance impact plastics, motor lubricant oil and adhesives [1–4]. Anionic polymerization was mostly used in industrially synthesizing styrene-butadiene block copolymers with different macromolecular architectures and composition. However, anionic polymerization required anhydrous and anaerobic reaction condition, and usually performed in solvent and lower temperature, which was restricted in the cost and environmental protection [5]. Reversible Addition-Fragmentation chain Transfer (RAFT) miniemulsion polymerization was an environmental friendly, energy saving and high efficiency for most monomers, which was considered to be one of the most prominent “living”/controlled free radical polymerization for both industrial and commercial perspectives [6–8]. In our previous work, preparation and nanoparticle structure of styrene-butadiene block copolymers via RAFT seeded miniemulsion polymerization mediated by different RAFT agents indicated that it was an efficient, controllable and environmentally friendly polymerization [9–11]. And other related research also mainly focused on synthesis and nanoparticles structure of the styrene-butadiene block copolymers for thermoplastic elastomers [12, 13]. Furthermore, styrene-butadiene diblock copolymers were the basic units for complex copolymers. Therefore, how to precisely produce the styrene/butadiene block with targeted composition and sequence length was very critical.

As we knew that different structure of styrene/butadiene block with targeted composition and structure was prepared in

Z. Wang · Q. Zhang (✉) · X. Zhan · F. Chen
Department of Chemical and Biological Engineering, Zhejiang University, Hangzhou 310027, People's Republic of China
e-mail: qh Zhang@zju.edu.cn

Z. Wang · G. Rao · J. Xiong
Institute of Energy Conversion, Jiangxi Academy of Sciences,
Nanchang 330096, People's Republic of China

anionic homogeneous polymerization by sequentially charging and monomer ratio change, which based on the kinetic model. Copolymerization kinetics is the only way to achieve targeted block composition copolymers. In RAFT retardation, fast fragmentation and irreversible termination mechanism played an important role to explain experimental phenomena [14, 15]. Thence, kinetic model for RAFT homogeneous polymerization was formulated, and produced copolymers with targeted composition and sequence [16]. Compared to a bulk or solution polymerization, more factors in the heterogeneous polymerization system such as the number of particles (N_p), number of propagating radical (\bar{n}) and monomers transport contributed to the RAFT heterogeneous miniemulsion polymerization kinetics [17]. So far, literatures about preparation and kinetic modeling for PS-b-PS/Bd diblock copolymers via RAFT miniemulsion copolymerization were not reported.

In this work, the binary monomers RAFT copolymerization kinetic models were formulated, and a series of PS-b-PS/Bd diblock copolymers with well-defined structure and composition were synthesized via RAFT seeded miniemulsion copolymerization, in which the modeling curves could well predict the experimental process. Additionally, gel fraction was reduced and avoided because of high monomers to polymers ratio in the miniemulsion nanoreactors [18]. The microstructure and the relationship between molecular structure and properties of the PS-b-PS/Bd diblock copolymers were investigated.

Theoretical development

It was well known that kinetics of emulsion or miniemulsion polymerization was described by the classical Smith-Ewart theory, which was obtained by population balance method. In general “0–1” case, the reaction rate was proportional both to the number of propagating radicals per particle and number of particles, which was expressed by Eq. (1).

$$-\frac{d[M]}{dt} = k_p \times N_p \times \frac{\bar{n}}{N_A} \times [M] \quad (1)$$

where $-\frac{d[M]}{dt}$ was reaction rate, k_p , N_p , \bar{n} , $[M]$ and N_A represented the propagation rate constant, the number of particles, average number of propagating radicals per particle, the monomer concentration and Avogadro constant, respectively.

The retardation effect was founded in RAFT bulk and miniemulsion polymerization system. The cross-termination reaction was attributed to the intermediate radicals with the propagating radicals in bulk RAFT polymerization [19]. However, in RAFT miniemulsion polymerization, Luo [17, 20] demonstrated that the most important factors contributing to the retardation in RAFT miniemulsion polymerization was the decrease in number of propagating radicals and particles.

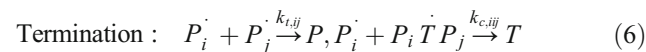
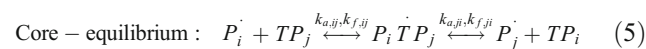
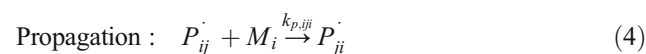
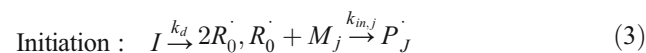
Based on the classic Smith-Ewart emulsion polymerization theory, the average number of propagating radicals for per particle was formulated by Eq. (2).

$$\frac{1}{\bar{n}_{RAFT}} = \frac{1}{\bar{n}_{blank}} + 2K[RAFT] \quad (2)$$

Where K was the RAFT equilibrium constant, which was ratio of the addition rate constant and the fragmentation rate constant in RAFT polymerization process. \bar{n}_{blank} and \bar{n}_{RAFT} were the average number of propagating radicals per particle in free RAFT and RAFT miniemulsion system, respectively.

The possible mechanism of binary monomers RAFT copolymerization was described in Scheme 1.

In Scheme 1, binary monomers RAFT elementary reactions were demonstrated as follow Eqs.(3)–(6), in which the copolymerization kinetics was identical to the terminal model.



During the binary monomers RAFT copolymerization reaction process, instantaneous different radical concentration was formulated by the binary monomers elementary reactions, and the total radical concentration was a constant approximately in steady state. The equilibrium coefficient $\langle K \rangle$ and propagation rate coefficient $\langle k_p \rangle$ were apparent [21], which were described as Eqs. (7)–(8).

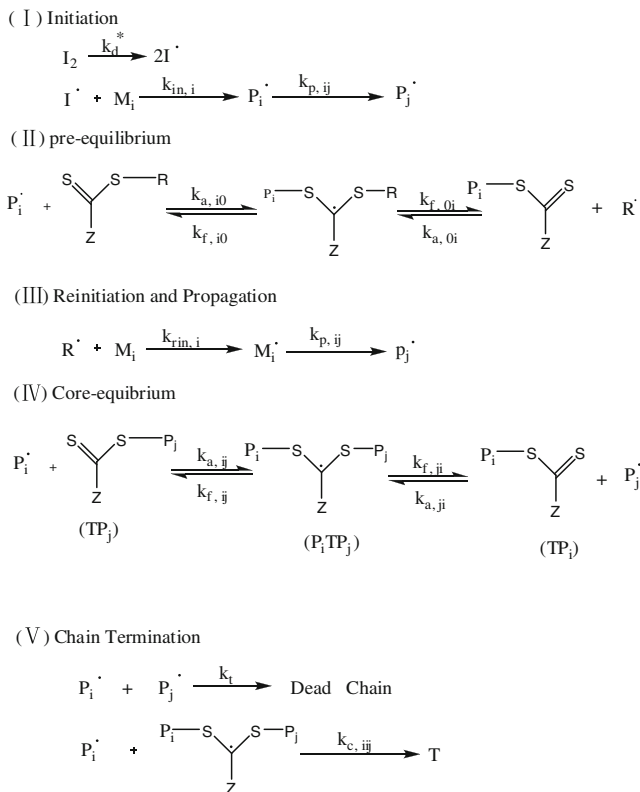
$$\langle K \rangle = \frac{r_1^2 f_1^2 k_{p,22}^2 K_{11}^2 + r_1 r_2 f_1 f_2 k_{p,11} k_{p,22} K_{11} K_{22} + r_2^2 f_2^2 k_{p,11}^2 K_{22}^2}{r_1^2 f_1^2 k_{p,22}^2 K_{11} + r_1 r_2 f_1 f_2 k_{p,11} k_{p,22} (K_{11} + K_{22}) + r_2^2 f_2^2 k_{p,11}^2 K_{22}} \quad (7)$$

$$\langle k_p \rangle = \frac{r_1 f_1^2 + 2f_1 f_2 + r_2 f_2^2}{\left(\frac{r_1 f_1}{k_{p,11}} + \frac{r_2 f_2}{k_{p,22}} \right)} \quad (8)$$

Where r_1 and r_2 were reactivity ratio for monomer 1 and 2, K_{11} and K_{22} were the homoequilibrium coefficients. f_1 and f_2 were molar fraction of monomers, which were expressed by Eqs.(9)–(10).

$$f_1 = \frac{[M_1]}{[M_1] + [M_2]} \quad (9)$$

$$f_2 = \frac{[M_2]}{[M_1] + [M_2]} \quad (10)$$



Scheme 1 Possible mechanism of binary monomers RAFT copolymerization

According to Mayo-Lewis theory, instantaneous molar fraction in the copolymer chains was expressed by Eqs. (11)–(12).

$$F_1 = \frac{r_1 f_1^2 + f_1 f_2}{r_1 f_1^2 + 2f_1 f_2 + r_2 f_2^2} \quad (11)$$

$$F_2 = \frac{r_2 f_2^2 + f_1 f_2}{r_1 f_1^2 + 2f_1 f_2 + r_2 f_2^2} \quad (12)$$

In this binary monomers RAFT copolymerization, such hypothesis was proposed. The number of particles in aqueous phase was a constant during the copolymerization process. When the particles average diameter was less than 300 nm, the double radicals termination has no effect on the copolymerization kinetics [22]. When monomers were swelled in batch reactor for a few hours, the whole monomers all migrated into particles before copolymerization. When monomer was continuous feeding in the reactor, and the volume fraction of monomers in the particles less than that of the critical phase equilibrium, monomers immediately migrated into particles to react with other monomers at the stirring rate.

In this case, feeding of styrene and butadiene was batch or continuous, in which 1 and 2 represented monomer of styrene and butadiene, respectively. During the copolymerization

process, instantaneous monomers concentration and volume of the particles were described by Eqs. (13)–(15).

$$\frac{d[M_1]}{dt} = \frac{D_1 \cdot \rho_{m,1}}{V} \cdot \frac{[M_1]}{V} \times \frac{dV}{dt} - F_{i,1} \cdot \langle k_p \rangle \cdot ([M_1] + [M_2]) \cdot \bar{n}_{RAFT} \cdot \frac{\bar{N}_p}{N_A} \cdot \frac{V_{seed}}{V} \quad (13)$$

$$\frac{d[M_2]}{dt} = \frac{D_2 \cdot \rho_{m,2}}{V} \cdot \frac{[M_2]}{V} \times \frac{dV}{dt} - F_{i,2} \cdot \langle k_p \rangle \cdot ([M_1] + [M_2]) \cdot \bar{n}_{RAFT} \cdot \frac{\bar{N}_p}{N_A} \cdot \frac{V_{seed}}{V} \quad (14)$$

$$\frac{dV}{dt} = D_1 + D_2 - V \times \left[R_1 \times \left(\frac{1}{\rho_{m,1}} - \frac{1}{\rho_{p,1}} \right) + R_2 \times \left(\frac{1}{\rho_{m,2}} - \frac{1}{\rho_{p,2}} \right) \right] \quad (15)$$

Where D , ρ and V , R_1 and R_2 represented feeding rate, density, volume of particles and reaction rate for monomer 1 and 2, m and p were monomer and copolymer, respectively.

As long as the initial conditions were given, which was labeled by 0, the sequence equations can be solved numerically using the “ODE45” routine in MATLAB. The instantaneous monomers’ concentration and volume of the particles could be obtained. Then kinetics could be calculated during the RAFT binary monomers copolymerization process, such as instantaneous monomers conversion, number-average molecular weight and the total molar fraction in the copolymer chains, which were expressed by Eqs. (16)–(20).

$$x_1 = 1 - \frac{[M_1] \cdot V}{[M_1]_0 \cdot V_0 + D_1 \cdot t \cdot \rho_{m,1}} \quad (16)$$

$$x_2 = 1 - \frac{[M_2] \cdot V}{[M_2]_0 \cdot V_0 + D_2 \cdot t \cdot \rho_{m,2}} \quad (17)$$

$$M_n = \frac{M_1 \cdot ([M_1]_0 \cdot V_0 + D_1 \cdot t \cdot \rho_{m,1}) \cdot x_1 + M_2 \cdot ([M_2]_0 \cdot V_0 + D_2 \cdot t \cdot \rho_{m,2}) \cdot x_2}{[RAFT]_0} + M_{RAFT} \quad (18)$$

$$F_{n,1} = \frac{([M_1]_0 \cdot V_0 + \rho_{m,1} \cdot D_1 \cdot t) \cdot x_1}{([M_1]_0 \cdot V_0 + \rho_{m,1} \cdot D_1 \cdot t) \cdot x_1 + ([M_2]_0 \cdot V_0 + \rho_{m,2} \cdot D_2 \cdot t) \cdot x_2} \quad (19)$$

$$F_{n,2} = \frac{([M_2]_0 \cdot V_0 + \rho_{m,2} \cdot D_2 \cdot t) \cdot x_2}{([M_1]_0 \cdot V_0 + \rho_{m,1} \cdot D_1 \cdot t) \cdot x_1 + ([M_2]_0 \cdot V_0 + \rho_{m,2} \cdot D_2 \cdot t) \cdot x_2} \quad (20)$$

Experimental

Materials

Deionized water (conductivity $< 4 \mu\text{S/cm}$) was used as received. Styrene (S, Sinopharm Chemical Reagent Co) was purified by reduced pressure distillation under $40 \text{ }^\circ\text{C}$. Butadiene (Bd, Qilu Petrochemical Co) was distilled directly from a 2.0 L stainless storage vessel into a cooling one at $-18 \text{ }^\circ\text{C}$. Hexadecane (HD, costabilizer, $> 99 \%$, from Aldrich), potassium persulfate (KPS,

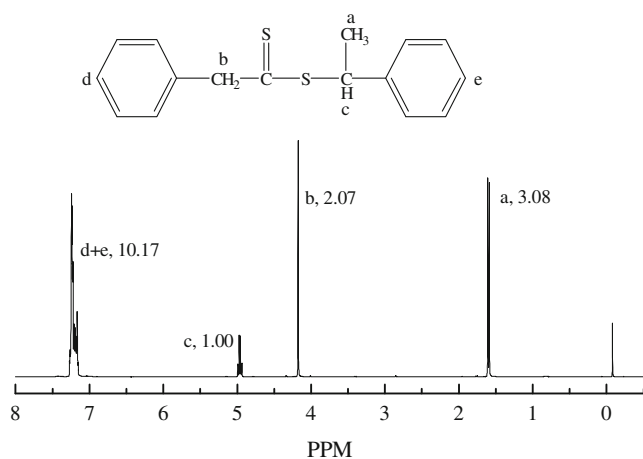


Fig. 1 $^1\text{H-NMR}$ Spectrum of PEPDTA

initiator, >99 %), sodium dodecyl sulfate (SDS, emulsifier, >99 %) and hydroquinone from Sinopharm Chemical Reagent Co. were used without further purification. 1-phenylethyl phenyldithioacetate (PEPDTA, RAFT agent) was synthesized and purified as previous reported [23], which was characterized by hydrogen nuclear magnetic resonance spectroscopy ($^1\text{H-NMR}$). In Fig. 1, the chemical shifts and peak integral of the protons in PEPDTA were in good agreement with the target molecular structure.

Styrene RAFT miniemulsion polymerization seeds

The homogeneous mixture of organic phase including styrene, 1-phenylethyl phenyldithioacetate were mixed and stirred for 15.0 min, in which the recipes were listed in Table 1. Then, aqueous solution of sodium dodecyl sulfate was added to the organic phase and stirred for 20 min. The heterogeneous mixture was homogenized by ultrasonic cell crusher at the amplitude of 70 % output in ice batch for 120 s. The styrene miniemulsion droplets whose particles average size was less than 100 nm were obtained. The resultant seeds miniemulsion

was charged into a 1,000 mL stainless reactor equipped with mechanical stirrer, nitrogen inlet, thermometer and sampling syringe, which was purged with nitrogen for about 15.0 min at 0 °C. Aqueous potassium persulfate solution was injected into the reactor to initiate the polymerization and kept the reaction temperature at 70 °C. When molecular weight of the polystyrene block increased to designed value, reaction stopped by decreasing the reaction to 0 °C, and sample was withdrawn.

Estimate the \bar{n}_{blank} and K_{Bd}

Butadiene RAFT miniemulsion polymerization was carried out, styrene miniemulsion droplets as seeds. When styrene polymerization completed, butadiene was injected into the stainless reactor through high pressure pump under 0 °C, and swelling about 4 h, then increasing the reaction temperature to 70 °C. The experimental recipes were listed in Table 2, in which Run 1–5 was used to determinate the RAFT equilibrium constant between butadiene with PEPDTA, and Run 6 was to determinate the average number of propagating radicals per particles in free RAFT miniemulsion polymerization system by additional initiator KPS based on additional amount of monomers.

Synthesis of PS-b-PS/Bd diblock copolymers

In order to synthesize different composition and molecular weight of the styrene/butadiene block, especially tapered or uniformed, two types of feeding method were taken. The first one was different amount of additional styrene and butadiene were swelling for about 4.0 h at 0 °C, then copolymerized with increasing temperature to 70 °C, which was batch feeding. The other was that additional styrene and small amount of butadiene were swelling at 0 °C, then increasing temperature to 70 °C. Then butadiene was continuously injected into the reactor at different flow rate through high pressure pump until the end of reaction, which was semibatch feeding. Experimental recipes were listed in Table 3, and samples were taken every hour.

Table 1 Recipes of styrene RAFT miniemulsion polymerization seeds

Run	S/g	Water/g	SDS/g	HD/g	PEPDTA/g	KPS/g	Reaction time/hour
1	80.0	740.0	4.0	4.0	0	0.312	4.0
2	80.0	740.0	4.0	4.0	0.48	0.312	4.0
3	80.0	740.0	4.0	4.0	0.95	0.312	4.0
4	80.0	740.0	4.0	4.0	1.30	0.312	4.0
5	80.0	740.0	4.0	4.0	1.60	0.312	4.0
6	80.0	740.0	4.0	4.0	0	0.312	4.0
7	80.0	740.0	4.0	4.0	0.90	0.312	1.5
8	80.0	740.0	4.0	4.0	1.30	0.312	2.5
9	80.0	740.0	4.0	4.0	1.45	0.312	2.0
10	80.0	740.0	4.0	4.0	1.60	0.312	3.0

Table 2 Recipes of butadiene RAFT miniemulsion polymerization

Run	Butadiene/ml	Additional KPS/g	Reaction time/hour
1	80.0	0	3.0
2	80.0	0	4.0
3	80.0	0	4.0
4	80.0	0	4.0
5	80.0	0	4.0
6	220.0	0.34 ^a	6.0

^a By 0.05 % or 0.02 % of additional monomer in batch or semibatch polymerization, mol

Characterization

Conversion of monomers was measured by gravimetry. Gel permeation chromatography (GPC, Waters 1525/2414) was used to determine molecular weight and molecular weight distribution of the samples. Composition of the copolymers and molecular structure of PEPDTA were characterized by hydrogen nuclear magnetic resonance spectroscopy (¹H-NMR, Bruker, 400 M), and the molar fraction of butadiene in the copolymers was calculated from Eq. (21).

$$F_{Bd} = \frac{5R - 3A}{5R + 3A} \tag{21}$$

In which, A was the proton peak integral of benzene ring, and R was the proton peak integral of butadiene and aliphatic chains. And in term of self-consistent field theory [24], microphase morphology of the copolymer could be predicted theoretically from the relation between thermodynamic parameter χN and volume fraction Φ , which was calculated from the molecular weight and composition by GPC and ¹H-NMR.

Fourier translation infrared spectroscopy (FT-IR, Nicolet5700) was used to identify the addition structure of butadiene including 1,4-*trans* units, 1,4-*cis* units and 1,2-units according to their the characteristic peaks [25]. The particle size of miniemulsion droplet was measured by dynamic light

Table 3 Recipes of styrene/butadiene RAFT miniemulsion polymerization

Run	Additional styrene/g	Additional KPS/g ^a	Butadiene		Reaction time/hour
			Batch	Semibatch ^b	
7	0	0.34	220.0	0	8.0
8	40.0	0.38	220.0	0	8.0
9	0	0.10	0	15.0	8.0
10	20.0	0.12	25.0	25.0	8.0

^a By 0.05 % or 0.02 % of additional monomer in batch or semibatch polymerization, mol

^b At the flow rate, ml/hour

Table 4 Model parameters

Parameter	Value	Reference
$k_{p,1}(L/mol \times s)$	$2.2 \times 10^7 \times \exp(-3.26 \times 10^4/RT)$	[26]
$k_{p,2}(L/mol \times s)$	$1.2 \times 10^8 \times \exp(-3.89 \times 10^4/RT)$	[26]
r_1	1.03	[26]
r_2	1.41	[26]
$\rho_{m,1}(mol/L)$	8.7	[26]
$\rho_{p,1}(mol/L)$	9.9	[26]
$\rho_{m,2}(mol/L)$	11.48	[26, 27]
$\rho_{p,2}(mol/L)$	16.3	[26, 27]
$K_S(L/mol \times s)$	22.0	[17]
$K_{Bd}(L/mol \times s)$	18.3	this work

scattering(DLS, Malvern Instrument 3000HSA), then the number of particles ($N_p/L H_2O$) was derived from Eq. (22).

$$N_p = \frac{6M_0}{\pi(\bar{D}_v)^3 \rho} \tag{22}$$

Where M_0 , \bar{D}_v and ρ represented monomer and polymer's concentration, weight average particle size and density of the droplets, respectively.

Transmission electron microscopy (TEM) was used to observe the morphologies of the copolymers. The final 5 wt.% copolymers of Run 7~10 dissolved in toluene solutions evaporated slowly for about two weeks at room temperature, under static conditions close to thermodynamic equilibrium. And the resulting films, ca. 0.3 mm thick, were dried for 4.0 h under vacuum at 60 °C and annealed for 24.0 h at 100 °C. Ultrathin sections, ca. 40~80 nm for TEM observation were obtained, cut with a diamond knife at -100 °C on a Leica Ultracut cryo-microtome. These sections were collected

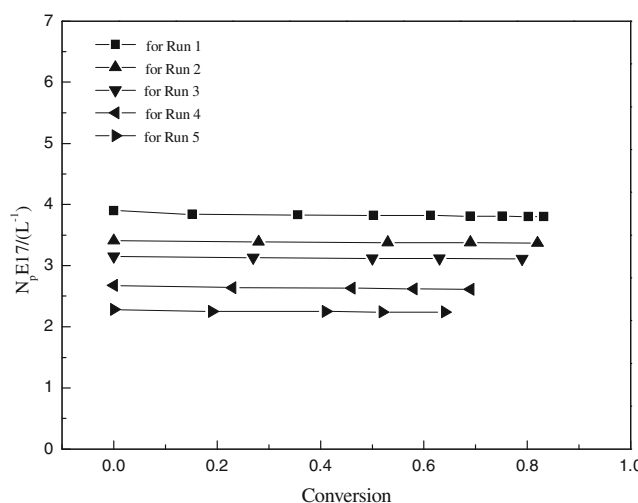
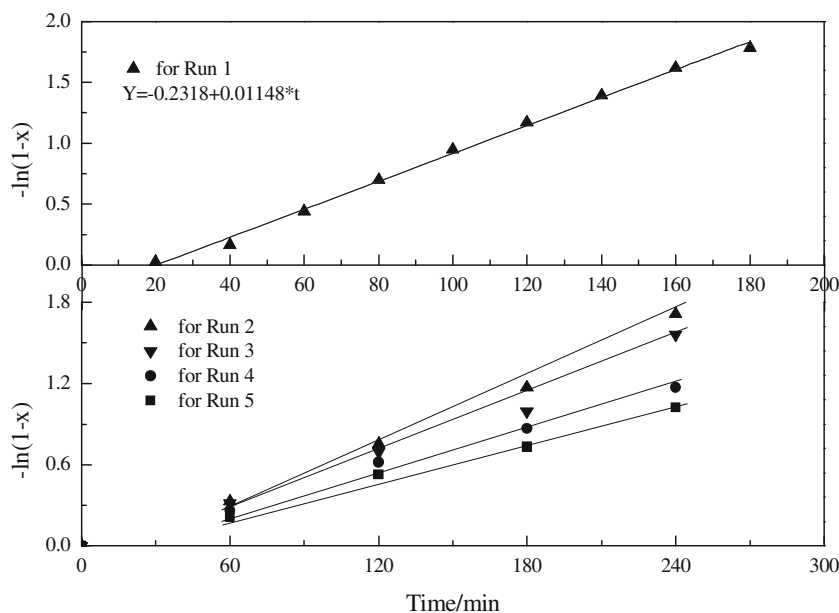


Fig. 2 Evolution of N_p vs. Bd conversion for Run1~5

Fig. 3 The polymerization index ($-\ln(1-x)$) vs. time for Run 1~5



on 400 mesh copper grids and exposed to Osmium tetroxide (OsO_4) vapors for about 45.0 min. Transmission electron micrographs were obtained on JEM-1230 operated at 80 kV.

The glass transition temperature of the copolymers was determined by differential scanning calorimetry (DSC) on TA instrument equipped with DSC Q100 module. The thermal history of samples was removed by annealing with keeping the temperature at 120 °C for 5 min, then they were cooled to -120 °C at the cooling rate of 40 °C/min. Therefore, samples were scanned from -120 to 120 °C with the heating rate of 10 °C/min.

Results and discussion

Binary monomers RAFT miniemulsion copolymerization kinetic models were formulated. Feeding methods based on the models could precisely controllably produce the copolymers

with different molecular structures. And kinetic parameters used in the modeling were listed in Table 4.

Kinetic parameters identification in Bd RAFT miniemulsion polymerization

The number of particles was a key parameter in S/Bd RAFT miniemulsion copolymerization, and butadiene RAFT miniemulsion polymerization kinetics were very importantly basic experiments for identification the average number of propagating radical per particle $\bar{n}_{p,\text{exp}}$ and the RAFT equilibrium constant K used in the kinetic model.

Changes in the number of particles

When styrene miniemulsion polymerized for 4.0 h in Run 1~6, conversion of styrene was about 0.95. It was considered that styrene polymerization completed due to thermodynamic control. Under the previous swelling conditions, butadiene

Table 5 The experimental data for Run 1~6

Run	\bar{D}_v/nm	\bar{N}_p/L	$V_{particles}/L$	$V_{emulsion}/L$	$-d \ln(1-x)/dt$	$\bar{n}_{p,\text{exp}}$
1	76.1	3.83E17	0.171	0.93	0.01148	0.37
2	79.3	3.38E17	0.171	0.93	0.0088	0.32
3	81.3	3.12E17	0.171	0.93	0.0074	0.29
4	86.2	2.62E17	0.171	0.93	0.0057	0.27
5	90.8	2.24E17	0.171	0.93	0.0045	0.24
6	85.0	2.60E17	0.310	1.05	0.0056	0.425

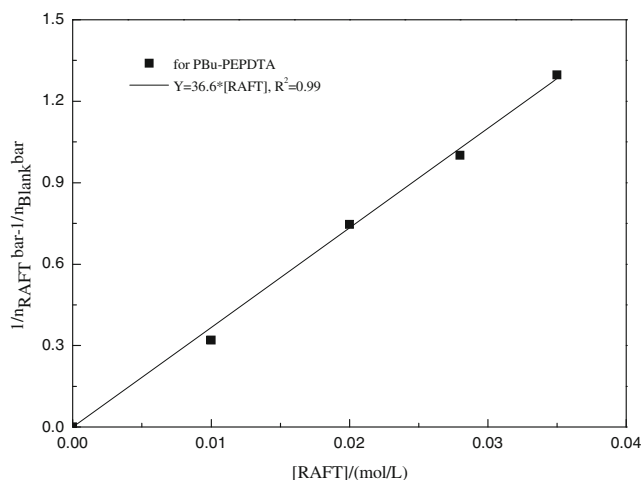


Fig. 4 Plot of \bar{n} vs. [RAFT] to estimate the equilibrium constant

monomer all diffused into the seeded droplets. Then increasing the reaction temperature to 70 °C, butadiene RAFT miniemulsion polymerization was carried out. Changes in the number of particles in Run 1~5 was studied by relationship between particles size and monomers' conversion (Eq. 22) during the polymerization process, which was shown in Fig. 2, where $N_p E 17$ was the meaning of $N_p \times 10^{17}$ in the Y axis.

In this series of experiments, the higher PEPDTA concentration in the droplets, the larger particles size, the number of particles in per liter was less in Run1~5, which was accounted for the effect of superswelling in the seeds early nucleation. With butadiene conversion increase, the number of particles per liter gradually decreased, but the reduced fraction was less than 5 %. Based on above experimental results and analysis, the effects of secondary nucleation and coalescence were negligible in butadiene RAFT miniemulsion polymerization.

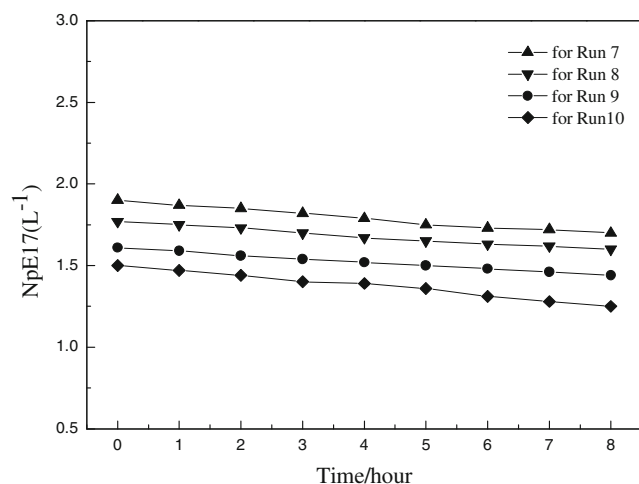


Fig. 5 Evolution of N_p vs. Bd conversion for Run7~10

Kinetics of butadiene RAFT miniemulsion polymerization

Butadiene RAFT miniemulsion polymerization with different PEPDTA concentration in Run1~5 was performed. The relationship between the polymerization index ($-\ln(1-x)$) and reaction time was shown in Fig. 3. Comparing Run 1 with the others, it was RAFT free miniemulsion polymerization, and reaction rate was faster than the others, therefore sampling interval was 20.0 min. In Run 1, it was clearly shown that the polymerization index ($-\ln(1-x)$) increased linearly with reaction time, when reaction for 3.0 h butadiene conversion was 0.83 with a small amount of gel. In Run2~5, with RAFT concentration increasing, the polymerization index decreased, which was mainly contributed to the decrease in N_p and \bar{n}_p . Figure 3 showed that was first order reaction, which meaning the characteristics of “living”/controlled radical polymerization.

Estimate of $\bar{n}_{p,exp}$ and K

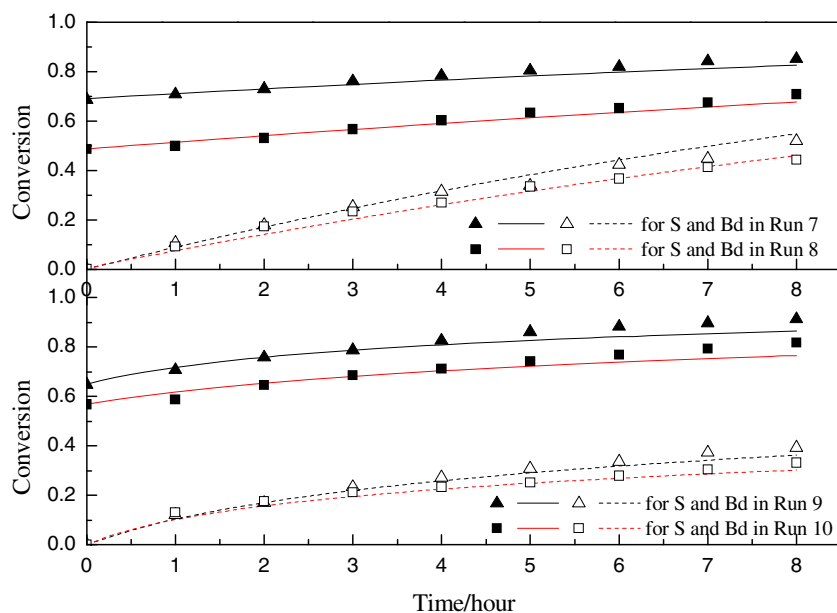
The average number of propagating radical per particle $\bar{n}_{p,exp}$ and the RAFT equilibrium constant K were important kinetic parameters, which was characterized the initiation rate and the ratio of addition and fragmentation coefficient between RAFT agent and monomer. In the semibatch seeded miniemulsion polymerization process, the decomposition rate of the initiator k_d decreased gradually with increasing the reaction time, although it was a constant within its half-life. In Run 1~5, the remaining KPS in the reactor reinitiated butadiene polymerization after the seeds polymerization completed. However, the reaction rate is reduced since the consumption of the initiator in butadiene polymerization process, while the reaction time longer, the emulsion instability and severe gelation happened. Therefore, during the butadiene polymerization process, additional initiator based on the monomer weight ratio was necessary. The average number of propagating radical per particle $\bar{n}_{p,exp}$ in Run 1~6 was calculated by Eq. (23).

$$\bar{n}_{p,exp} = \frac{-\frac{d\ln(1-x)}{dt} \times N_A \times V_{particles}}{60 \times k_p \times \bar{N}_p \times V_{emulsion}} \quad (23)$$

The average number of propagating radical per particle $\bar{n}_{p,exp}$ listed in Table 5.

From Tab. 5, it was found that the polymerization index and the average number of propagating radical per particle decreased with increasing RAFT concentration in the same conditions for Run 1~5, which was in good agreement with our previous works [28]. In Run 6, the average number of propagating radical per particle $\bar{n}_{p,exp}$ for butadiene free RAFT miniemulsion polymerization was 0.425, which was the average number of propagating radical per particle slightly lower than that of styrene free RAFT miniemulsion

Fig. 6 Monomers conversion of experiment and simulation vs. time for Run 7~10



polymerization 0.43 [28], because of the solubility of styrene greater than that of butadiene in aqueous phase. According to “0–1” case in the classic Smith-Ewart theory [27], the average number of propagating radical per particle was described by Eq. (24).

$$\bar{n} = \frac{\rho}{2\rho + k} \quad (24)$$

Where ρ and k were the entry rate coefficient and the exit rate coefficient, respectively. The value of \bar{n} was less than 0.5, which was consistent with the theoretical. In copolymerization experiment simulation process, the average number of propagating radical per particle \bar{n}_p as 0.43 was taken.

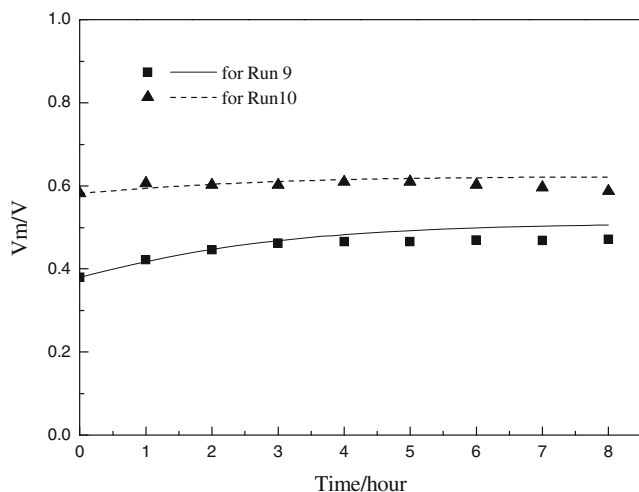


Fig. 7 The volume ratio of monomers in particles vs. time for Run 9~10

According to RAFT mechanism, miniemulsion polymerization kinetics was a very suitable method for estimation the RAFT equilibrium constant, while the RAFT equilibrium constant for butadiene was estimated by Eq.(2). And plots of $\bar{n}_{RAFT}^{-1} - \bar{n}_{blank}^{-1}$ versus $[RAFT]$ was shown in Fig. 4, in which slope of the fitted line was to estimate the RAFT equilibrium constant for butadiene polymerization mediated by PEPDTA.

In Fig. 4, the fitted line was $Y = 36.6 \times [RAFT]$ with $R^2 = 0.99$, therefore the RAFT equilibrium constant K for butadiene polymerization mediated by PEPDTA was $18.3 L/mol \times s$ in $70^\circ C$.

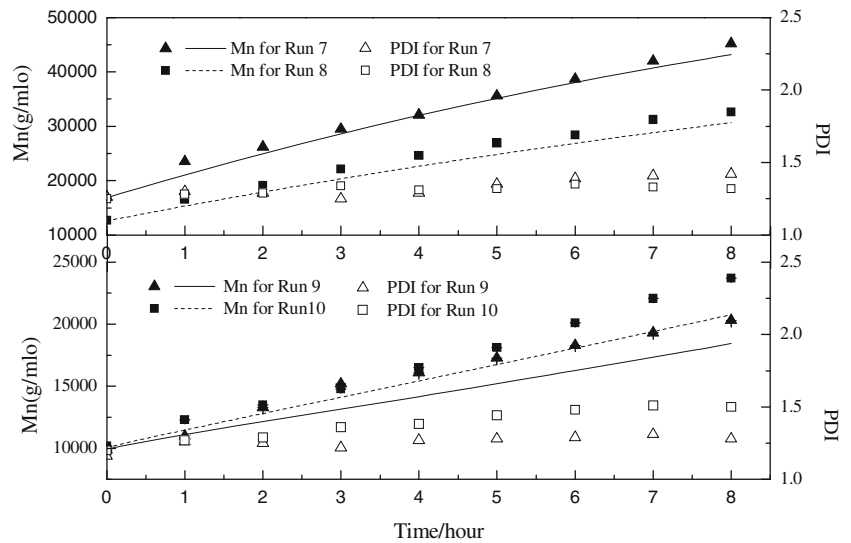
Kinetics of S/Bd copolymerization

Based on the formulated models, styrene/butadiene RAFT miniemulsion copolymerization kinetics were identified, which including the number of particles, monomers conversion, volume fraction of monomers in particles, M_n with its distribution(PDI), and composition.

The number of particles for S/Bd copolymerization

In Run7~10, the number of particles in per liter was shown in Fig. 5. As can be seen that N_p decreased with increase PEPDTA concentration and reaction time, which was in good agreement with the previous works for Run 1~5. However, the N_p decreased slightly, which has little effect on the polymerization kinetics simulation. Therefore, the initial value of S/Bd seeded miniemulsion was considered as a constant during the copolymerization process, when secondary nucleation and coalescence effect on polymerization kinetics were ignored.

Fig. 8 M_n of experiment and simulation vs. time for Run 7~10



Monomers conversion

In Run 7~10, the two former and two latter trials were batch and semibatch seeded miniemulsion polymerization, respectively. It was shown that the theoretic modeling curves formulated in Eq. (16)–(17) were approaching to the experimental data in Fig. 6. Later in S/Bd copolymerization, the experimental data of monomers conversion were slightly higher than that of modeling curves. The main reason for this deviation between experiment and modeling may be that the particles viscosity increased with monomers fraction decrease and small amount of particles coalescence. In the whole S/Bd seeded RAFT miniemulsion polymerization, the kinetic models well predicted the experiment processes.

Volume fraction of monomers

In emulsion polymerization I and II stage, the volume fraction of monomers in particles was a constant because of

thermodynamic balance between the mixed and interfacial energy. According to the literature [29], the volume fraction of styrene and butadiene were 0.604 and 0.592 in emulsion polymerization, respectively. Therefore, monomers instantaneously diffused into the seeded particles in semibatch experiments, when the volume fraction of monomers was less than about 0.60. During butadiene semibatch feeding process, the volume fraction of monomers in Run 9~10 was shown in Fig. 7.

As could be seen that the volume fraction of monomers in Run 9 is less than 0.50 in Fig. 7, and that of Run 10 is slightly lower than 0.60. Late in polymerization, experimental data is below the modeling curve because of monomers conversion deviation. During the semibatch polymerization process, the volume fraction of monomers was below the critical point. Therefore, butadiene instantaneously diffused into the seeded particles to react together with other monomers.

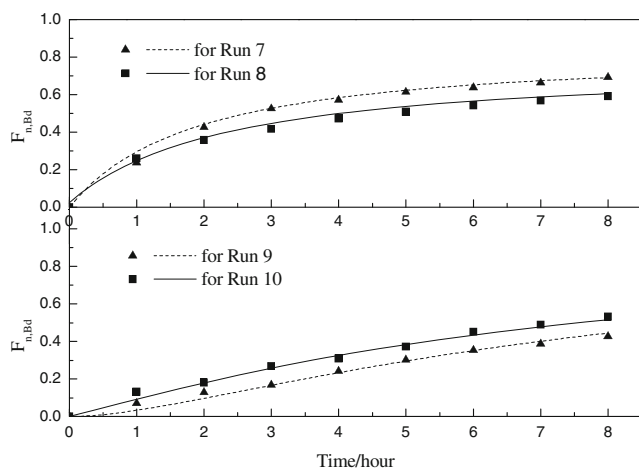


Fig. 9 Molar fraction of Bd in the copolymers vs. time for Run 7~10

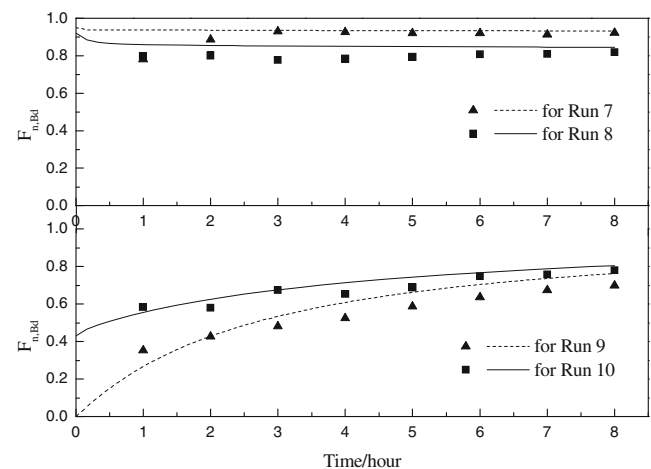


Fig. 10 Molar fraction of Bd in S/Bd block vs. time for Run 7~10

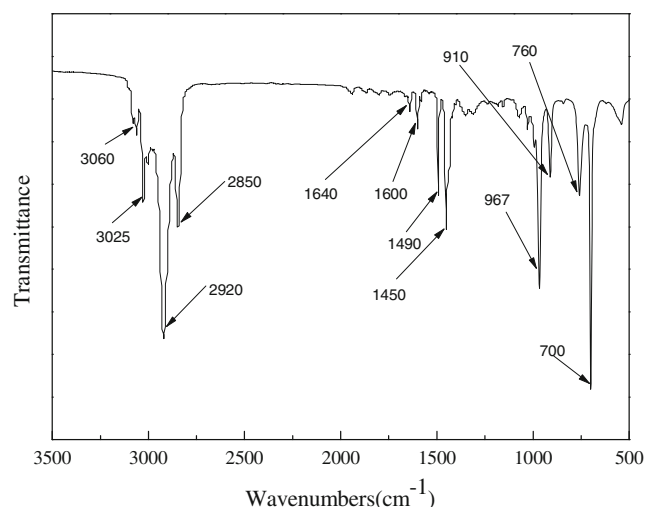


Fig. 11 FT-IR spectrum of PS-b-PS/Bd diblock copolymers for sample 7

M_n and PDI of the PS-b-PS/Bd copolymers

Number-average molecular weight (M_n) and its distribution (PDI) of the copolymers were shown in Fig. 8. It was found that M_n of the experiment increased linearly along with the increasing of time, which was close to the kinetic modeling curves with narrow distribution described in Eq.(18), meaning the characteristics of “living”/controlled radical polymerization. Along with time, PDI of the copolymers gradually increased about from 1.20 to 1.50, due to the increase of “dead” chains. Additionally, gel fraction was not obviously observed even at high conversions, because of high monomers to polymers ratio in the miniemulsion nanoreactors.

Composition of the PS-b-PS/Bd copolymers

Composition and sequence of individual copolymer chains was controlled by programmed feeding. Different composition and sequence copolymers was obtained by semibatch feeding polies, such as uniformed, gradient or tapered composition

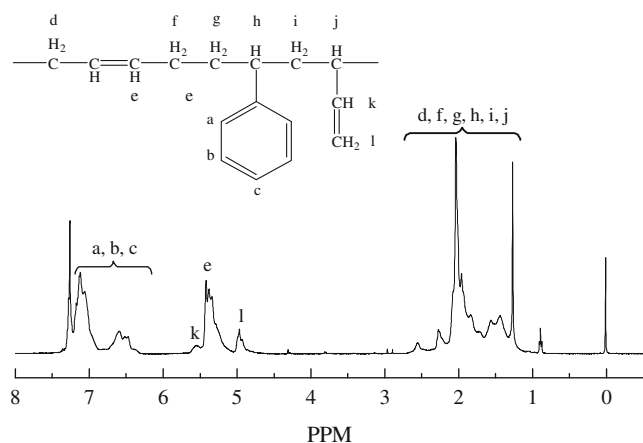


Fig. 12 $^1\text{H-NMR}$ spectrum of PS-b-PS/Bd diblock copolymers for sample 7

profiles. Composition and sequence in the PS-b-PS/Bd and PS/Bd block of the copolymer chains was tailored.

Cumulative composition of the copolymers Butadiene molar fraction in PS-b-PS/Bd copolymer chains was shown in Fig. 9 for Run 7~10. It was the result that the composition of butadiene for experimental characterization was in good agreement with the modeling curves for Run 7~10. As one of the most important targets to predict composition of the copolymers was an effective polymerization method based on the feeding strategy formulated by the kinetic models. It was evident in Fig. 9 that butadiene composition profiles formulated by kinetic models well predicted that in styrene/butadiene RAFT seeded batch or semibatch miniemulsion copolymerization.

Composition of the S/Bd block in the copolymers Butadiene molar fraction of PS/Bd block in PS-b-PS/Bd copolymer chains was calculated by molecular weight of the first block PS, diblock PS-b-PS/Bd copolymer chains and butadiene molar fraction in the copolymers both for experiment and modeling curves. Butadiene molar fraction in PS/Bd block was shown in Fig. 10. The results showed that composition profiles with a constant lines and curves were formulated by the kinetic models. From Fig. 10, it was indicated that different copolymer chains structure with uniformed and gradient or tapered composition were controllably synthesized by batch or semibatch feeding strategy based on the kinetic models. And the deviation between the experimental data and the modeling curves was mainly due to small amount of dead chains. During the copolymerization process, molar fraction of Bd in S/Bd block was close to the modeling curves in the copolymer chains.

Microstructure, microphase morphology and thermal property of the copolymers

The produced copolymer chains structure was characterization by FT-IR and $^1\text{H-NMR}$ spectrum. microphase morphology and thermal property of the products was studied by TEM and DSC.

Molecular microstructure of the copolymers

According to FT-IR spectrum of sample 7 in Fig. 11, the characteristic peaks of 1,4-*trans* units' stretching band at 760 and 967 cm^{-1} , and 1,2-units' stretching band at 910 cm^{-1} were observed, but the characteristic peaks at 724 and 1,650 cm^{-1} of 1,4-*cis* units were not observed obviously. And other peaks were shown that where 700 cm^{-1} was the peak of hydrogen atoms on the benzene ring bending vibration, the peaks of 1,450 and 1,490 cm^{-1} were C-H bending vibration. Where 1,600 cm^{-1} was the peak of benzene

Table 6 Molecular characteristics of PS-*b*-PS/Bu diblock copolymers

Sample	N_{total}	N_{S1}	F_S	$x_{S,S/Bd}$	χ_{eff}	Φ_{PS}	$\chi_{eff} N_{total}$	Morphology ^a
7	651	164	0.31	0.0784	0.037	0.425	24.1	L
8	438	123	0.41	0.1816	0.029	0.533	12.7	C
9	246	95	0.57	0.3001	0.022	0.685	5.5	DIS
10	306	99	0.47	0.2200	0.027	0.593	8.3	DIS

$$F_S = N_S/N_{total}, x_{S,S/Bd} = \frac{F_S N - N_1 - N_2}{N - N_1 - N_2}, \chi_{eff} = (1 - x_{S,S/Bd})^2 \chi_{S/Bd}, \chi_{S/Bd} = 6.59 \times 10^{-3} + 13.6/T$$

^a L lamellae; C cylinders; DIS disordered phase

vibration, 1,640 cm⁻¹ was the peak of C=C in the copolymers. The peaks of 2,800~3,000 and 3,000~3,100 cm⁻¹ were C-H in the benzene bending vibration and stretching vibration, respectively. Moreover, that of other samples was almost in the same. It was suggested that the structure of butadiene in the copolymer chains mainly should be 1, 4-*trans* and 1, 2-units.

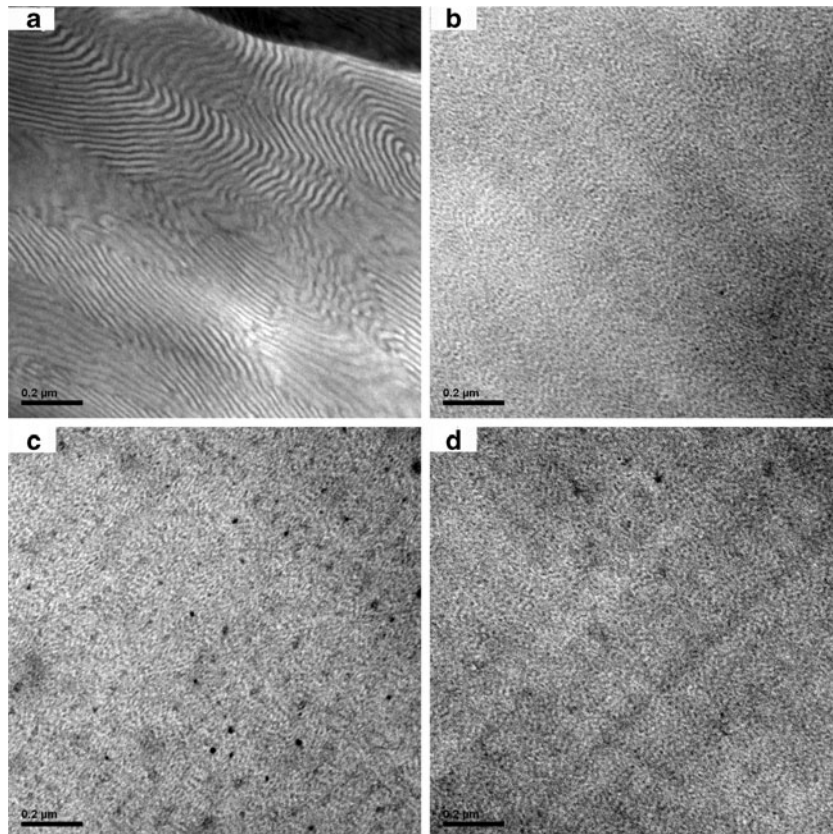
¹H-NMR was used to identify content of butadiene and proportion of 1, 4-*trans*, and 1, 2-butadiene in the copolymers. Figure 12 was ¹H-NMR spectrum of sample 7 dissolved in CDCl₃, which was representative of all samples. According to ¹H-NMR spectrum, the peak at $\delta=6.4\sim 7.1$ ppm range corresponded only to the protons of styrene (H_a, H_b and H_c), and the peak at $\delta=5.3\sim 5.4$ ppm range represented the protons

of 1, 4-butadiene double bond (H_e), and two peaks at about $\delta=4.9$ ppm and 5.5 ppm related to protons of 1, 2-butadiene double bond (H_i and H_k), while $\delta=1.2\sim 2.5$ ppm range belonged to the protons of methyl and methylene (H_d, H_f, H_g, H_h, H_j and H_l) in the ¹H-NMR spectrum. FT-IR and ¹H-NMR results indicated that microstructure of the copolymers was mainly 1, 4-*trans* butadiene with 10 % content of 1, 2-units, and copolymers composition was obtained.

Microphase morphology of the copolymers

Difference in cohesive energy density of units in copolymer chains, microphase separation with long range order structure appeared thermodynamically. According to thermodynamics

Fig. 13 TEM micrographs of PS-*b*-PS/Bu diblock copolymers: **a** for sample 7, **b** for sample 8, **c** for sample 9, and **d** for sample 10



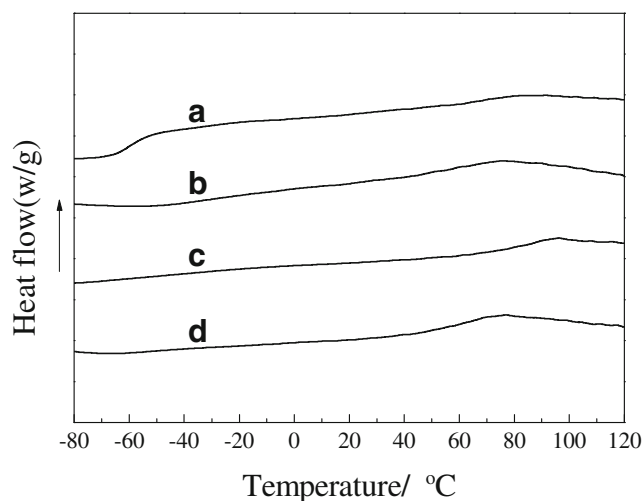


Fig. 14 DSC heating traces of PS-b-PS/Bd diblock copolymers: **a** for sample 7, **b** for sample 8, **c** for sample 9, and **d** for sample 10

theory, the main contribution were enthalpy and entropy contribution to the free energy density, which was defined as χ and N^{-1} . χN was an important thermodynamic parameter in the equilibrium state of block copolymers. According to references [24, 30, 31], styrene/butadiene block copolymers thermodynamic parameters were listed in Table 6, and microphase morphologies of the copolymers by TEM were shown in Fig. 13, which produced by RAFT batch or semibatch miniemulsion polymerization.

Where N_{total} and N_{S1} were the statistical units of the copolymers and styrene, F_S was the molar fraction of styrene units in the copolymers, and χ_{eff} was the interaction parameter between the PS and PBd segregation, respectively.

In terms of the self-consistent field theory calculations on basis of relationship between volume fraction ϕ and combination parameters χN [32], it could precisely predict diblock copolymers morphology in thermodynamic phase diagram. In Table 6, morphology of sample 7 and 8 could be lamellar and cylinder morphology, and the others could be disordered phase, as predicted by self-consistent field theory. And further studies were to identify the microstructure of the copolymers by TEM, which was shown in Fig. 13.

From Fig. 13, as could be seen that in picture a, the lamellae microphase separation structure was very clear, and the width of the two phases was uniformed, in which the white and black areas were polystyrene and polybutadiene aggregate. And in picture b, polybutadiene aggregate uniformly embedded in the polystyrene aggregate areas with cylinders microstructures. While the others of sample 9 and 10 were not clear in corresponding microphase separation structure, it was in disordered phase due to its lower molecular chains. TEM identification results indicated that morphology of the copolymers was consistent with the self-consistent field theory prediction in thermodynamic equilibrium phase.

Thermal properties of the produced copolymers

The glass transition behaviors of the programmed feeding produced copolymers for Run 7~10 were studied by DSC. The DSC heating traces of the final copolymers for Sample 7~10 were shown in Fig. 14. As can be seen that two glass transition temperature(Tg) behaviors exhibited in the $-80\sim 0$ °C and $0\sim 120$ °C range for Sample a and b. For Sample a, two Tg were about -50 and 75 °C, and for b, that were about -15 and 65 °C, respectively. In sample a and b, the S/Bd block in the copolymer chains were uniformed, and the butadiene composition of sample a was greater than that of sample b, while the molecular weight of the first PS block was larger than that of sample b. This was the cause of glass transition behaviors and microphase separation. While in sample c and d, there were not obvious Tg in the $-80\sim 0$ °C range, only a single Tg were 90 and 65 °C of each sample, as the result of PS content. The S/Bd block composition of c and d were gradient or tapered, and the chain length was relatively less, which cause a wide range of glass transition behaviors and weak microphase separation.

Conclusion

In this work, binary monomers RAFT miniemulsion copolymerization kinetic modeling was developed to predict and produce PS-b-PS/Bd copolymers with different well-defined structure and composition for controlled RAFT radical copolymerization. In butadiene RAFT miniemulsion polymerization, the number of particles and the polymerization index ($-\ln(1-x)\sim t$) was almost a constant. And the RAFT equilibrium constant between butadiene and PEPDTA was estimated, which was $18.3L/mol \times s$ under this reaction conditions. During styrene/butadiene RAFT miniemulsion copolymerization process, the experimental data of monomers conversion, volume fraction of monomers, number-average molecular weight and composition were in good agreement with the modeling curves, which indicated the models could well predict styrene/butadiene copolymerization kinetics. The copolymers molecular structure were characterized by FT-IR, 1H -NMR. The results showed that the copolymers was mainly 1, 4-*trans* butadiene with 10 % content of 1, 2-units. Microphase morphologies and thermal properties of the copolymers were identical to their microphase separation, sequence length and composition by TEM and DSC.

Acknowledgments The authors gratefully thank the financial support from the National Natural Science Foundation of China (21276224, 21176212 and 51303074), Program for Science and Technology Funds of Jiangxi Province (20123BBE50113 and 2008GQC0060), and the Research Funds of Jiangxi Academy of Sciences (2013XTPH1-13, 2012-02 and 2011-YYB-06).

References

- Liu IC, Tsiang RC (2003) Method of determining the absolute molecular weight from gel permeation chromatograms for star-shaped styrenic block copolymers. *J Polym Sci A Polym Chem* 41: 976–983
- Jouenne S, Gonzalez-Len JA, Ruzette AV, Lodefier P, Leibler L (2008) Styrene-butadiene gradient block copolymers for transparent impact polystyrene. *Macromolecules* 41:9823–9830
- Radhakrishnan CK, Kumari P, Sujith A, Unnikrishnan G (2008) Dynamic mechanical properties of styrene butadiene rubber and poly (ethylene-co-vinyl acetate) blends. *J Polym Res* 15:161–171
- Zhang HY, Zhang XY (2009) Synthesis and characterization of miktoarm star copolymer of styrene and butadiene using multifunctional macromolecular initiator. *Chin Chem Lett* 20:1131–1135
- Hadjichristidis N, Iatrou H, Pispas S, Pitsikalis M (2000) Anionic polymerization: high vacuum techniques. *J Polym Sci A Polym Chem* 38:3211–3234
- Brouwer H, Tsavalas JG, Schork FJ, Monteiro MJ (2000) Living radical polymerization in miniemulsion using reversible addition-fragmentation chain transfer. *Macromolecules* 33:9239–9246
- Moad G, Rizzardo E, Thang SH (2012) Living Radical Polymerization by the RAFT Process. *Aust J Chem* 65:985–1076
- Yang L, Qiu SJ, Zhang Y, Xu YS (2013) Preparation of PDMS/SiO₂ nanocomposites *via* ultrasonical modification and miniemulsion polymerization. *J Polym Res* 20:68
- Wang ZX, Zhang QH, Zhan XL, Yu YT, Chen FQ, Xiong JH (2010) Synthesis of polystyrenes-styrene/butadiene diblock copolymers *via* reversible addition-fragmentation chain transfer miniemulsion polymerization. *Chin Chem Lett* 21:1497–1500
- Yu YT, Zhang QH, Wang ZX, Zhan XL, Chen FQ (2012) Synthesis of surface-functionalized poly(styrene-co-butadiene) nanoparticles *via* controlled/living radical mini-emulsion copolymerization stabilized by ammonolyzed poly(styrene-alt-maleic anhydride) (SMA) RAFT agent. *J Macromol Sci A* 49:60–66
- Yu YT, Zhang QH, Zhan XL, Chen FQ (2013) Interfacially confined RAFT miniemulsion copolymerization of styrene and butadiene. *J Appl Polym Sci* 127(4):2557–2565
- Wei RZ, Luo YW, Li ZS (2010) Synthesis of structured nanoparticles of styrene/butadiene block copolymers *via* RAFT seeded emulsion polymerization. *Polymer* 51(17):3879–3886
- Wei RZ, Luo YW, Zeng W, Wang FZ, Xu SH (2012) Styrene-butadiene-styrene triblock copolymer latex *via* reversible addition-fragmentation chain transfer miniemulsion polymerization. *Ind Eng Chem Res* 51:15530–15535
- Monteiro MJ, Brouwer H (2001) Intermediate radical termination as the mechanism for retardation in reversible addition-fragmentation chain transfer polymerization. *Macromolecules* 34:349–352
- Wang CX, Xu J, Gao Y, Yang DG, Li HM (2012) RAFT synthesis of acrylic polymers containing diol or dioxane groups. *J Polym Res* 19:9895
- Sun XY, Luo YW, Wang R, Li BG, Zhu SP (2008) Semibatch RAFT polymerization for producing ST/BA copolymers with controlled gradient composition profiles. *AIChE J* 54:1073–1087
- Luo YW, Wang R, Li BG, Zhu SP (2006) Effect of reversible addition fragmentation transfer (RAFT) reactions on (mini)emulsion polymerization kinetics and estimate of RAFT equilibrium constant. *Macromolecules* 39:1328–1337
- Kohnle MV, Ziener U, Landfester K (2009) Synthesis of styrene – butadiene rubber latex *via* miniemulsion copolymerization. *Colloid Polym Sci* 287:259–268
- Kwak Y, Goto A, Fukuda T (2004) Rate retardation in reversible addition-fragmentation chain transfer (RAFT) polymerization: further evidence for cross-termination producing 3-arm star chain. *Macromolecules* 37:1219–1225
- Luo YW, Tsavalas JG, Schork FJ (2001) Theoretical aspect of particle swelling in ‘living’ free radical miniemulsion polymerization. *Macromolecules* 34:5501–5507
- Gao J, Luo YW, Wang R, Li BG, Zhu SP (2007) Kinetics of methyl methacrylate and n-butyl acrylate copolymerization mediated by 2-cyanoprop-2-yl dithiobenzoate as a RAFT agent. *J Polym Sci A Polym Chem* 45:3098–3111
- Tobita H (2009) RAFT miniemulsion polymerization kinetics, 1–polymerization rate. *Macromol Theor Simul* 18:108–119
- Quinn JF, Rizzardo E, Davis TP (2001) Ambient temperature reversible addition-fragmentation chain transfer polymerization. *Chem Commun* 11:1044–1045
- Roe RJ, Zin WC (1980) Determination of the polymer-polymer interaction parameter for the polystyrene-polybutadiene pair. *Macromolecules* 13:1221–1228
- Zeng XR (2007) Gao fen zi jin dai ce shi fen xi ji shu (Modern Analytical Techniques of Polymer, in Chinese). Guangzhou: South China University of Technology Press, P83,141
- Pan ZR (2003) Gao fen zi hua xue (Polymer chemistry, in Chinese, the third edition), Beijing: Chemical Industry Press, P39, 89
- Weerts PA, German AL, Gilbert RG (1991) Kinetic aspects of the emulsion polymerization of butadiene. *Macromolecules* 24:1622–1628
- Wang ZX, Zhang QH, Zhan XL, Chen FQ (2010) Kinetics of styrene reversible addition-fragmentation chain transfer polymerization. *CIESC Journal* 61(4):854–860
- Meehan EJ (1949) Variation of monomer pressure with degree of conversion in emulsion polymerization of butadiene and of butadiene-styrene. *J Am Chem Soc* 71:628–633
- Sakurai S, Mori K, Okawara A, Kimishima K, Hashimoto T (1992) Evaluation of segmental interaction by small-angle X-ray scattering based on the random-phase approximation for asymmetric, polydisperse triblock copolymers. *Macromolecules* 25:2679–2691
- Jouenne S, González-León JA, Ruzette AV, Lodefier P, Tencé-Girault S, Leibler L (2007) Styrene/butadiene gradient block copolymers: molecular and mesoscopic structures. *Macromolecules* 40:2432–2442
- Matsen MW, Bates FS (1996) Unifying weak and strong-segregation block copolymer theories. *Macromolecules* 29:1091–1098